

## Pigment Mutants of the Green Microalga *Chlamydomonas reinhardtii*: Morphological Properties and Photosynthetic Performance

A. K. Sadvakasova<sup>a</sup>, N. R. Akmukhanova<sup>a</sup>, B. K. Zayadan<sup>a</sup>, D. N. Matorin<sup>b</sup>, F. F. Protopopov<sup>b,c</sup>,  
A. A. Alekseev<sup>c</sup>, and K. Bolatkhan<sup>a</sup>

<sup>a</sup> Faculty of Biology and Biotechnology, Al-Farabi Kazakh National University,  
ul. Timiryazeva 71, Almaty, 050040 Republic of Kazakhstan

<sup>b</sup> Faculty of Biology, Moscow State University, Moscow, Russia

<sup>c</sup> North-Eastern Federal University, ul. Belinskogo 58, Yakutsk, 677000 Russia  
e-mail: sadvakasova1979@mail.ru

Received December 7, 2015

**Abstract**—Pigment mutants CC-124y-1, CC-124y-2, and CC-124p-2 of the green microalga *Chlamydomonas reinhardtii* Dangeard were obtained by means of UV-induced mutagenesis. Morphological properties and photosynthetic activity of these mutants were examined. The mutants displayed a lowered content of chlorophyll *b* and carotenoids. Analysis of fluorescence induction curves revealed the decreased rates of electron transport in photosystem II (PSII), the increase in the fraction of Q<sub>B</sub>-nonreducing centers, and the enhancement of nonphotochemical fluorescence quenching. The mutations had no direct impact on oxidation of pigment P<sub>700</sub> in PSI and on the decline of delayed fluorescence. The parameters of induction curves of prompt and delayed fluorescence are proposed for use in early diagnostics of UV-induced mutagenesis. The pigment mutants obtained can be applied in biomonitoring studies.

**Keywords:** *Chlamydomonas reinhardtii*, chlorophyll *a* fluorescence, delayed fluorescence, JIP test, photosynthesis

**DOI:** 10.1134/S1021443716040130

### INTRODUCTION

The modern trend in biomonitoring is the use of various test specimens for bioassays. Biological testing is a rapid diagnostic technique for assessing toxicity of aquatic environments. This method, combined with the analysis of genetic material stability under the influence of anthropogenic load, permits the timely detection of environmental mutagenic factors, thus helping to alleviate the adverse action of mutagens on living organisms [1]. The methodology of present-day genetic monitoring is based on efficient and fast-operating test systems for assessing the genetic disorders caused by environmental factors. It is, thus, important to search for new prospective test organisms for predicting genetic consequences of environmental factors and to study ecological and biological features of these organisms.

**Abbreviations:** Chl—chlorophyll(s); DF—delayed fluorescence; FNR—ferredoxin—NADP reductase; O, J, I, P—intermediate steps in the fluorescence induction curve; P<sub>700</sub>—reaction center pigment in PSI; PAR—photosynthetically active radiation; PF—prompt fluorescence; PQ—plastoquinone; Q<sub>A</sub> and Q<sub>B</sub>—primary and secondary quinone acceptors of electrons; RC—reaction center.

Microalgae represent a convenient model system for studying the impact of various (e.g., mutagenic) factors on populations and photosynthetic activity [2]. The green unicellular alga *Chlamydomonas reinhardtii* Dangeard is a useful model organism in genetics. Studying the influence of mutagenic substances on the wild-type and mutant strains not only unveils the biological effects of pollutants but also offers promising test systems for genetic monitoring of the environment. Bioassays of aquatic environments using pigment mutants are advantageous, because they reveal not only toxicity but also the potential mutagenicity of contaminated waters. For example, the yellow mutant strain is suitable for biotests of water quality, since the detection of revertants with the original green color can be used in diagnostics of aquatic ecosystems for the presence of mutagens.

The aims of this work were to obtain mutant strains of *C. reinhardtii*, to characterize their morphology, and to apply spectral and fluorescence methods for assessing the photosynthetic performance of algae at early stages of the mutation process.

## MATERIALS AND METHODS

The mutants of the green microalgae *Chlamydomonas reinhardtii* Dangeard were obtained using UV-B irradiation (254 nm, 4 J/m<sup>2</sup>). The 5-day-old cells of *C. reinhardtii* were suspended in water. The suspension was poured into a sterilized petri dish, which was then subjected to irradiation with UV-B light and transferred onto petri dishes filled with the L2-min medium [3]. Petri dishes were placed in darkness for 24 h to prevent photoreactivation [3]. Next, the inoculated petri dishes were exposed to photosynthetically active radiation (PAR, 120 μmol/(m<sup>2</sup> s); after 10–14 days of cell growth, the results were evaluated. We performed up to ten sequential cycles of selection using artificial light of quartz halogen lamps. Genetic studies on *Chlamydomonas* were performed with the method of macrocolonies and microcolonies [4].

The induction curves of prompt and delayed chlorophyll (Chl) fluorescence (PF and DF) and the redox conversions of P<sub>700</sub> were measured with a Multi-Function Plant Efficiency Analyzer (M-PEA-2, Hansatech Instruments, United Kingdom) intended for simultaneous measurements of all three parameters [5–7]. The kinetics of PF and DF were measured under alteration of red light pulses (1300 μmol/(m<sup>2</sup> s), peak emission at 627 nm) and short dark intervals sufficient for DF detection. The kinetics of fluorescence induction was measured with the highest resolution of 10 μs. The absorbance changes at 820 nm are assumed to reflect the redox state of chlorophyll P<sub>700</sub> in the reaction centers (RCs) of photosystem I (PSI). The intensity of modulated light peaking at 820 ± 25 nm was 1000 μmol/(m<sup>2</sup> s). The reflectance data at 820 nm were normalized to reflectance at *t* = 0.7 ms (termed thereafter as MR<sub>0</sub>) [6]. The duration of each measurement was 60 s. The DF kinetics reflected changes in emission intensity on a time scale of 0.1–0.9 ms in the intervals between actinic light pulses. Characteristics and the protocol of measurements with an M-PEA-2 instrument have been described in detail previously [6, 8, 9].

Prior to measurements, the algal samples were concentrated on a membrane filter and kept in darkness for 10 min in wet condition. This procedure of sample preparation was considered as the control treatment. It should be noted that M-PEA-2 analyzer is optimized for measurements with plant leaves. Because of high density of immobilized algal cells sedimented on filters, the signal-to-noise ratio in the records was as high as in measurements with leaves. The average chlorophyll content in the cells pelleted on filters was ~400 mg/m<sup>2</sup>, which was comparable to its content in leaves of vascular plants (approximately 500 mg/m<sup>2</sup>) [10]. Control measurements of fluorescence on cell suspensions of *Scenedesmus quadricauda* using an Aqua-Pen-C (AP-C 100) fluorometer (Photon Systems Instruments, Czech Republic) have shown that the procedure of concen-

trating samples on filters had no influence on cell physiological condition [9].

Quantitative analysis of the primary events in photosynthesis was performed using the so-called JIP-test based on OJIP parameters of the fluorescence induction [5, 6, 11]. The JIP-test includes the following parameters of the fluorescence induction curve: fluorescence intensity at 20 μs (*F*<sub>0</sub>), 2 ms (*F*<sub>J</sub>), 30 ms (*F*<sub>I</sub>), 6 s (*F*<sub>6s</sub>), and *F*<sub>P</sub> (*F*<sub>M</sub>); the maximum variable fluorescence (*F*<sub>V</sub>); and *M*<sub>O</sub> (the area above the OJIP fluorescence transient and below the maximum fluorescence *F*<sub>M</sub>).

These measured values were used for calculating the following parameters [5, 6]:

$F_V = F_M - F_O$ —the maximum variable fluorescence;

$F_V/F_M$ —the maximal quantum yield of primary photochemical reaction in open RCs of PSII:  $F_V/F_M = \varphi_{P_0} = TR_O/ABS$ ;

*V*<sub>J</sub>—relative variable fluorescence at the O–J transition:  $V_J = (F_J - F_O)/F_V$ ; it reflects the proportion of Q<sub>B</sub>-nonreducing centers in PSII;

*V*<sub>I</sub>—relative variable fluorescence at the J–I transient; it characterizes the reduction level of the quinone pool and the ability of PSI and its acceptors to oxidize PQH<sub>2</sub>:  $V_I = (F_I - F_O)/F_V$ ;

$\varphi_{E_0}$ —quantum efficiency of electron transfer from Q<sub>A</sub><sup>-</sup> (at *t* = 0):  $\varphi_{E_0} = ET_O/ABS = (TR_O/ABS) (ET_O/TR_O) = 1 - (F_O/F_M) (1 - V_J)$ ;

$\varphi_{D_0}$ —quantum efficiency of energy dissipation:  $\varphi_{D_0} = 1 - \varphi_{P_0} = (F_O/F_M)$ ;

ABS/RC—energy flux absorbed by one active RC; it characterizes the relative size of the antenna:  $ABS/RC = (TR_O/RC)/(TR_O/ABS) = M_O/V_J(1/\varphi_{P_0}) = (M_O/V_J)/[(F_M - F_O)/F_M]$ ;

PI<sub>ABS</sub>—performance index, a measure of PSII functional activity normalized to absorbed energy:  $PI_{ABS} = [1 - (F_O/F_M)]/(M_O/V_J) [(F_M - F_O)/F_O] [(1 - V_J)/V_J]$ ;

PI<sub>total</sub>—the overall performance index, a measure of functional activity of PSII, PSI, and the intersystem electron transport:  $PI_{total} = PI_{ABS} \delta_{R_0}/(1 - \delta_{R_0})$ ;

q<sub>E</sub>—pH-induced nonphotochemical fluorescence quenching:  $q_E = (F_M - F_{6s})/F_V$ ;

q<sub>PQ</sub>—fluorescence quenching by the quinone pool:  $q_{PQ} = (F_M - F_I)/F_V$ .

The absorption spectra were measured with a dual-wavelength spectrophotometer Hitachi 557 (Hitachi, Japan). Fluorescence spectra of algae were recorded with a spectrofluorometer Fluorolog®-3 (Horiba Jobin Yvon SAS, France) equipped with the time correlated single photon counting (TCSPC) option. Fluorescence was excited with a light-emitting diode in the spectral range 390–700 nm and was measured at 685 nm.

All measurements were performed at least in five replicates. Data in figures are the means of at least three replicate measurements.

## RESULTS

### *UV-Induced Mutagenesis and Selection of Mutant Clones*

In order to obtain any mutations, appropriate mutagen doses ensuring a high percentage of mutants at relatively high survival rates should be determined. Consequently, the lethal and mutagenic effects of the mutagen applied at various doses should be examined.

The study with a wild-type *C. reinhardtii* strain CC-124 has shown that UV-B irradiation strongly diminished the rates of cell survival. After 1-min irradiation, the number of surviving cells was 31%; the developed colonies differed inconspicuously from the control group: they had the same mean size and green color.

The UV-B irradiation for 2 min reduced the number of surviving cells to 10.5%. The newly grown colonies were heterogeneous in size and color (large, medium, and very small colonies of green, light-green, and deep-green color).

After 3-min irradiation, the number of surviving cells was 4–5%. The algal colonies had various dimensions and were mostly dark-green. After 5-min irradiation, no colonies of microalgae survived. The low viability of cells at high irradiation doses indicates a strong damaging effect of UV-B light. Our data suggest that prolonged exposure to UV-B with a wavelength of 254 nm and intensity of 4 J/m<sup>2</sup> had a lethal effect on *Chlamydomonas* cells.

We found that irradiation of *C. reinhardtii* strain CC-124 with UV-B light for 1–3 min reduced the cell survival rates and provided appropriate conditions for the appearance of mutations with distinct phenotypic traits. It should be noted that the mutants were identified not immediately after irradiation but after a 24-h recovery period, because the frequency of mutations in the latter case was elevated by errors in DNA replication.

Using various culture conditions and selection of colonies (without genotype verification), we obtained the subclones comprising the colonies of different sizes and color. These subclones were divided into six groups.

*In photoautotrophic culture conditions*, four groups were distinguished. Group 1: green subclones of a large size (A), 18% of the total number of colonies; group 2: green subclones of microscopic dimensions (B), 32%; group 3: light-green subclones of medium size (C), 33%; and group 4: yellow subclones of medium size (D), 17%.

*In heterotrophic culture conditions*, two distinct groups were found. Group 5: light-green subclones of

medium size (E), 68% of the total number; and group 6: yellow subclones of medium size (F), 32%.

The control group consisted of green medium size colonies.

The highest frequency of mutations was observed after 2-min irradiation with UV-B light (Table 1).

Analysis of the abundance of various mutant subclones in photoautotrophic culture conditions revealed the prevalence (up to 33% of total number) of light-green medium size subclones. Under heterotrophic conditions, light-green medium size subclones were prevalent and constituted up to 68% of the total number of mutant subclones.

Thus, when the wild-type strain of *C. reinhardtii* was exposed for 1–3 min to UV-B radiation (254 nm, 4 J/m<sup>2</sup>), 12056 subclones survived out of 130000 cells in the initial sample. Using these colonies, we selected 12 mutant subclones for further research; they were subjected to further selection, with up to ten consecutive cycles. In all experiments aimed at selection of *C. reinhardtii* mutant subclones, the L2-min nutrient medium was always used. Subclones were selected based on their ability to restore growth and retain the acquired phenotypic traits for a series of passages. Using the multiple selection method and the 12 subclones representing groups 3–5, we finally selected three colonies that retained the traits acquired during the induced mutagenesis.

The light-green pigment mutant obtained under photoautotrophic conditions was designated as CC-124y-1. The light-green and yellow pigment mutants obtained under heterotrophic conditions were designated as CC-124y-2 and CC-124p-2, respectively.

All these strains were similar in growth–morphological characteristics and did not differ significantly in terms of colony size and color. The cells of CC-124y-1 and CC-124p-2 strains were 2.0–3.5 μm in size. When grown on a solid nutrient medium, these cells formed light-green colonies, whereas the cells of CC-124y-2 were 3.0–3.5 μm in size and formed yellow colonies. All cells of these strains had two flagella of equal length that were located at the front end of the cell. Chlorophyll was entirely confined within chromatophores. The cells grew well at air temperature of 22–30°C in liquid and agarized L2-min nutrient media in photoautotrophic conditions.

### *Photosynthetic Activity of the Pigment Mutant CC-124y-1*

The strains CC-124y-2 and CC-124 were similar in spectral and fluorescent parameters. Figure 1 shows the absorption spectra of wild-type *C. reinhardtii* cells and of the mutant strain CC-124y-1. These spectra were normalized to the red maximum of Chl *a* absorption at 680 nm. In the mutant strain of CC-124y-1, compared with the wild type, a significant reduction in light absorption at 650 nm was observed, which

**Table 1.** Frequency of mutations in the wild-type CC-124 *Chlamydomonas reinhardtii* cells exposed to various doses of UV-B irradiation

| Duration of irradiation, min | Total number of colonies | Cell survival rate, % | Number of standard colonies | Number of mutant colonies | Designation of selected colonies |
|------------------------------|--------------------------|-----------------------|-----------------------------|---------------------------|----------------------------------|
| 0                            | 90000                    | 92–100                | 86000                       | —                         | —                                |
| 1                            | 39060                    | 31                    | 31248                       | 7812                      | A                                |
|                              |                          |                       |                             |                           | B                                |
| 2                            | 13230                    | 10.5                  | 8997                        | 4233                      | A                                |
|                              |                          |                       |                             |                           | B                                |
|                              |                          |                       |                             |                           | C                                |
|                              |                          |                       |                             |                           | D                                |
|                              |                          |                       |                             |                           | E                                |
|                              |                          |                       |                             |                           | F                                |
| 3                            | 5670                     | 4.5                   | 3629                        | 2041                      | E                                |
|                              |                          |                       |                             |                           | F                                |
| 5                            | —                        | —                     | —                           | —                         | —                                |

Colonies obtained under phototrophic conditions: A—green large subclones; B—green subclones of microscopic dimensions; C—light-green subclones of medium sizes; D—yellow subclones of medium dimensions. Colonies obtained under heterotrophic conditions: E—light-green medium-sized subclones; F—yellow medium-size subclones.

indicates a severalfold decrease in the content of Chl *b* compared to Chl *a*. This conclusion was also supported by measurements of fluorescence excitation spectra (Fig. 1b).

In absorption spectra of the mutant CC-124y-1, the absorbance of carotenoids at 470–480 nm was reduced (Fig. 1a). In the mutant strain, spectral changes attributed to carotenoids were even more pronounced in the fluorescence excitation spectra (Fig. 1b), which is an argument for a substantial deficiency of carotenoids in the mutant CC-124y-1.

It is known that carotenoids in algae do not emit fluorescence but effectively transfer the excitation energy to Chl *a*, the main source of fluorescence. In fluorescence excitation spectra of the mutant CC-124y-1, fluorescence intensity excited at 480–500 nm was reduced to a larger extent compared with changes in the absorption spectra, thus indicating a weak interaction of carotenoids and light-emitting Chl *a*.

Fluorescent methods of assessing the photosynthetic activity can provide detailed information on the primary disorders of cell metabolism, mainly at the membrane level [6, 7]. Furthermore, such methods

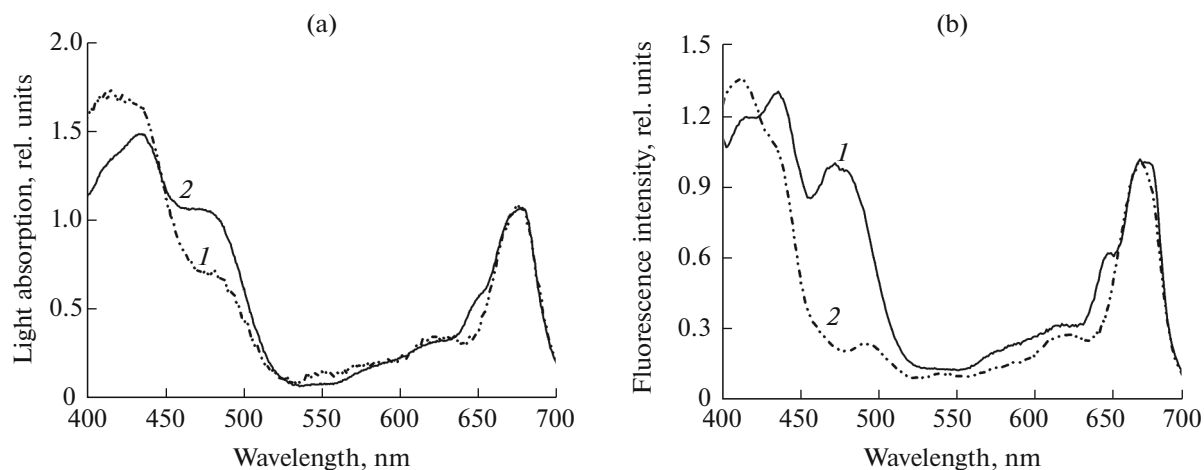


**Fig. 1.** Spectra of (a) light absorption and (b) fluorescence excitation for the wild-type *Chlamydomonas reinhardtii* CC-124 cells (1) and the mutant strain CC-124y-1 (2). Spectra were normalized to the red maximum of Chl *a* absorption at 680 nm.

**Table 2.** JIP-test parameters for fluorescence induction curves measured with the suspensions of wild-type strain CC-124 and the mutant strain CC-124y-1 of *Chlamydomonas reinhardtii*

| Parameter                    | CC-124            | CC-124y-1         | Definition  |
|------------------------------|-------------------|-------------------|---|
| $\Phi_{P_0}$ , ( $F_V/F_M$ ) | $0.728 \pm 0.017$ | $0.365 \pm 0.002$ | Maximum quantum yield of primary photochemistry, after dark adaptation  |
| $\Phi_{E_0}$                 | $0.353 \pm 0.004$ | $0.219 \pm 0.001$ | Quantum yield of electron transport beyond $Q_A^-$  |
| $\Phi_{D_0}$                 | $0.272 \pm 0.005$ | $0.635 \pm 0.01$  | Quantum yield of energy dissipation by the antenna complex (at $t = 0$ )                                      |
| ABS/RC                       | $1.485 \pm 0.014$ | $2.865 \pm 0.046$ | Absorption flux per RC (index reflecting RC concentration in the total Chl content)                           |
| $PI_{ABS}$                   | $1.695 \pm 0.023$ | $0.302 \pm 0.004$ | Performance index on absorption basis (indicator of PSII activity normalized to absorption of photons)        |
| $PI_{total}$                 | $1.505 \pm 0.010$ | $0.666 \pm 0.005$ | Total performance index (indicator of functional activities of PSII, PSI, and intersystem electron transport) |
| $q_E$                        | $0.177 \pm 0.004$ | $0.343 \pm 0.005$ | pH-induced nonphotochemical quenching of fluorescence   |
| $q_{PQ}$                     | $0.228 \pm 0.002$ | $0.413 \pm 0.003$ | Fluorescence quenching by the quinone pool  |

Kinetic curves of the fluorescence induction were measured with an M-PEA-2 analyzer under actinic illumination with a photon flux density of  $1300 \mu\text{mol}/(\text{m}^2 \text{ s})$  PAR.

provide information on the condition of the specimen in real time. Chlorophyll residing in photosynthetic membranes acts as an intrinsic indicator of the cell photosynthetic activity due to emission of fluorescence. The ratio of fluorescence yields at high irradiance that saturates photosynthesis ( $F_M$ ) and at low irradiance that has no influence on the functional state of photosynthetic apparatus ( $F_O$ ) is proportional to the maximum efficiency of PSII:  $(F_M - F_O)/F_M = F_V/F_M$ . The parameter  $F_V/F_M$  is a dimensionless energy characteristic that quantifies the photochemical efficiency of photosynthesis. The maximum quantum yield of primary photochemistry  $F_V/F_M$  ( $\Phi_{P_0}$ ) in the wild type of *C. reinhardtii* was as high as 0.728 (Table 2). By contrast, in the mutant strain CC-124y-1, the parameter  $F_V/F_M$  was lowered.

Measurements of fluorescence induction curves with a high temporal resolution (10  $\mu\text{s}$ ) under excitation with high intensity light have been increasingly used for assessment of the photosynthetic apparatus in higher plants and algae [5, 6]. High-resolution measurement of the fluorescence induction curve by means of PAM or PEA fluorimeters takes only a few seconds. The multifunctional analyzer M-PEA-2 offers the opportunity of simultaneous measurements of fluorescence and absorbance changes of  $P_{700}$ , the RC pigment of PSI. Thus, M-PEA-2 device permits simultaneous monitoring of PSII and PSI reactions [5–7]. Moreover, the M-PEA-2 also records the induction changes of delayed fluorescence.

For a detailed assessment of changes in photosynthetic activity of the mutants, we used M-PEA-2 to measure the induction parameters of prompt and delayed fluorescence and of the redox state of  $P_{700}$ .

Figure 2a shows the fluorescence induction curves that were normalized to the level O. In the wild-type cells, the fluorescence kinetics corresponded to those described in the literature [5, 11]. The kinetics of fluorescence induction in response to high-intensity light usually comprises several stages known as O-J-I-P transitions [5]. The initial level O corresponds to the Chl fluorescence intensity when the reaction centers in PSII are open and  $Q_A$  is fully oxidized. The phase O-J is caused by light-induced reduction of  $Q_A$ , whereas the subsequent phases are mainly due to further accumulation of reduced  $Q_A$  caused by its retarded reoxidation upon the reduction of the acceptor  $Q_B$  and the quinone pool.

Fluorescence induction curves obtained with the mutant strain CC-124y-1 differed from those of the wild-type strain (Fig. 2a). Variable fluorescence  $F_V$  ( $F_V = F_M - F_O$ ) was low in the mutant strain, reflecting primarily the decrease in  $F_M$ , which might be due to the enhanced nonphotochemical quenching [6].

The primary photosynthetic processes were quantified using the JIP-test (see Materials and Methods), which is based on the kinetic parameters of O-J-I-P curves (Table 2).

In the mutant strain CC-124y-1 the parameter ABS/RC was elevated (2.865), indicating the reduced proportion of active PSII RCs compared to that in the wild type (1.485).

The fraction of  $Q_B$ -nonreducing PSII centers ( $V_J$  parameter) was increased in the mutant strain, while the parameter  $\Phi_{E_0}$  reflecting the maximum quantum yield of electron transport to  $Q_A^-$  was reduced (Table 2). The highest quantum yield was observed in the wild-

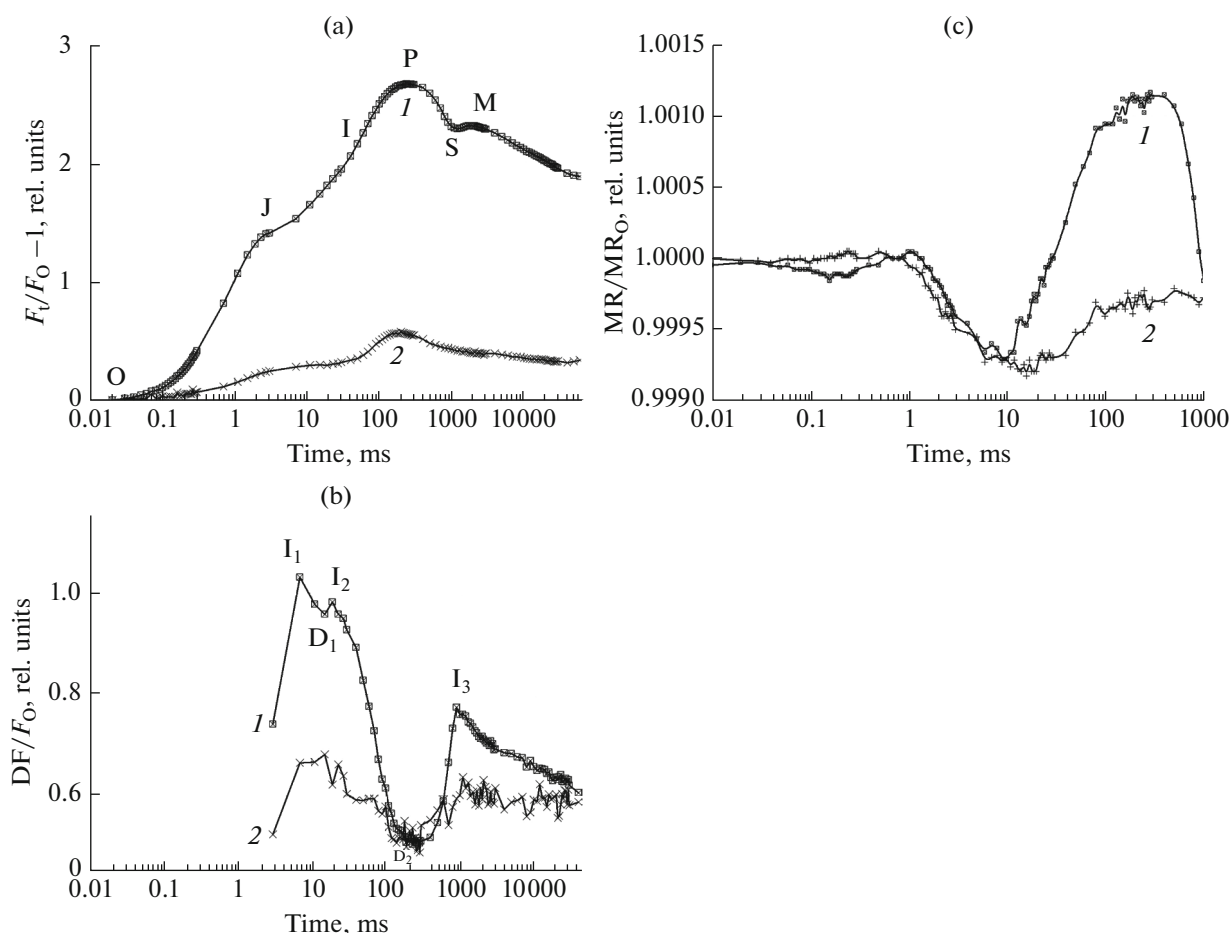


**Fig. 2.** Induction curves of (a) prompt fluorescence, (b) delayed fluorescence, and (c) absorbance changes at 820 nm in the wild-type cells of *Chlamydomonas reinhardtii* (CC-124) (1) and in the mutant strain CC-124y-1 (2). Delayed fluorescence was normalized to  $F_0$  ( $DF/F_0$ ). Photon flux density of actinic red light was 1300  $\mu\text{mol}/(\text{m}^2\text{s})$  PAR. All parameters were measured simultaneously using an M-PEA-2 analyzer.

type strain CC-124, whereas the mutant was characterized by low quantum efficiency. In the mutant CC-124y-1, the parameter  $V_1$  was also lowered, which presumably reflects the hindrance for electron transfer from PSII to the pool of “fast” plastoquinones (Table 2) [6]. In turn, this circumstance was largely caused by the decreased PSII activity, especially  $F_V/F_M$  and  $V_J$  parameters in the mutant.

The parameter  $PI_{\text{ABS}}$  is a measure of functional activity of PSII, normalized to the absorbed energy (ABS). High values of this parameter were noted in wild-type cells. Low values of  $PI_{\text{ABS}}$  in the mutant strain indicate the suppressed functional activity of PSII in relation to the low maximum quantum yield of PSII, caused probably by reduced abundance of active RCs and the increased proportion of  $Q_B$ -nonreducing centers.

The parameter  $PI_{\text{total}}$  (total performance index), like  $PI_{\text{ABS}}$  (performance index on the absorption basis), takes into account not only the functional activity of

PSII but also that of PSI and the activity of intersystem electron transport. Thus,  $PI_{\text{total}}$  is a very sensitive indicator and can also be used for the integrated assessment of photosynthetic performance.

The decline in efficiency of excitation energy transfer from the light-harvesting complex to RC should be accompanied by an increased dissipation of excess light energy. Indeed, the quantum efficiency of energy dissipation ( $\phi_{D_0}$ ) in the mutant CC-124y-1 was high (Table 2). This correlates with an increase in this mutant of  $\Delta\text{pH}$ -dependent nonphotochemical quenching qE, as calculated from the fluorescence decline after reaching the peak  $F_M$ :  $q_E = (F_M - F_{6s})/F_V$ . In addition, the quinone pool in the mutant CC-124y-1 had an increased ability to quench fluorescence on the I-P phase ( $q_{PQ}$ ).

Measurements of modulated reflectance at 820 nm in parallel with fluorescence changes revealed the photoinduced oxidation of chlorophyll  $P_{700}$  in the RCs of PSI, (with the maximal accumulation of  $P_{700}^+$  at  $t \approx$

of 30 ms), which was followed by  $P_{700}$  reduction (Fig. 2c). The fluorescence signal reflecting  $Q_A$  reduction reached the plateau almost synchronously with the  $P_{700}$  reduction. The parallel accumulation of the reduced forms of  $P_{700}$  and  $Q_A$  reflects the reduction of all intersystem carriers in the absence of electron outflow from the acceptor part of PSI in the conditions when ferredoxin–NADP reductase (FNR) is inactivated after dark incubation. The prolonged illumination (1–10 s) induced the second wave of  $P_{700}$  oxidation, which can be explained by the outflow of electrons from PSI upon activation of FNR and the Calvin cycle enzymes.

The mutant CC-124y-1 retained the ability to oxidize  $P_{700}$  upon illumination (Fig. 2c). However, the reduction of  $P_{700}$  by PSII was retarded, because of the reduced efficiency of PSII. This observation is consistent with the analysis of the induction curves of prompt fluorescence.

The millisecond DF component originates in the secondary recombination of charges and depends on the electrochemical proton gradient across the thylakoid membrane, because this gradient lowers the activation energy for charge recombination. Therefore, delayed fluorescence allows researchers to monitor changes in the proton gradient across thylakoid membranes. The maximum of DF in the millisecond range on the induction curve ( $I_1$ ) coincides in time with the J-I phase of fluorescence increase in the induction curve of prompt fluorescence (Fig. 2a). The peaks  $I_1$  and  $I_2$  are caused by accumulation of certain redox states (in varying proportions for submillisecond  $Z^+PQ_A^-Q_B^-$  and millisecond  $Z^+Q_A^-Q_B^-$  components) that are responsible for charge recombination and DF emission (i.e., light-emitting states). In addition, the peaks  $I_1$  and  $I_2$  result from the enhancement of DF by the transmembrane electric potential,  $\Delta\psi$ . The third DF peak  $I_3$  observed in the time range of seconds is associated with the photoinduced formation of the transmembrane proton gradient,  $\Delta pH$  [6], which also elevates the rate constant of light emission (DF) in PSII RCs. These issues were extensively considered in many works [5–7].

In the mutant strain CC-124y-1, the DF peaks on the induction curve were significantly reduced at the time frames of 10–50 ms (peaks  $I_1$  and  $I_2$ ) and ~1 s (peak  $I_3$ ) (Fig. 2b), which is probably associated with a significant retardation of noncyclic transport and the respective decrease in energization of photosynthetic membranes.

Thus, simultaneous recording of the induction curves for prompt and delayed fluorescence and  $P_{700}$  redox state using the M-PEA-2 analyzer allowed us to trace the reduction of some intersystem electron carriers, to detect the involvement of PSI, and to follow the kinetics of the electrochemical proton gradient in the thylakoid membrane of *Chlamydomonas* mutant strains.

## DISCUSSION

It is known that UV rays easily penetrate into the cells, thereby damaging DNA unique sites and causing various mutations [12]. Therefore, UV-B radiation is often used in studies on induced mutagenesis. The literature contains ample data showing that UV-B irradiation of cells can block pigments synthesis and retard cell growth [12, 13]. This notion gains further support from our study, in which the mutant subclones morphologically different from the control strain were obtained.

The pigment content is an integral index that determines not only the development and activity of the photosynthetic system but also the time course of many enzymatic reactions; i.e., it characterizes the productivity, viability, and resistance of plant organisms [14]. Irradiation with UV-B disrupts the functioning of plant pigment systems, disturbs the content and composition of pigments. UV-B irradiation of plant cells inhibits synthesis and promotes the photodestruction of Chl [14, 15]. The sensitivity of Chl *a* synthesis to mutagens of various origins was described [16]. At the same time, the influence of UV-B on Chl *b* is assumed to be weak and, accordingly, it is less investigated. The impact of UV-B is manifested in the reduced ratios of Chl *b*/Chl *a* and Chl/carotenoids [17].

The use of M-PEA-2 analyzer revealed changes in PSII operation and  $P_{700}$  oxidation in the mutant strain. Analysis of fluorescence induction curves revealed the retardation of electron transport in PSII, which was mainly caused by the decreased proportion of active RCs, decrease in  $F_V/F_M$  ratio, the increased number of  $Q_B$ -nonreducing centers, and the enhancement of  $\Delta pH$ -dependent nonphotochemical quenching. In addition, energization of photosynthetic membranes was found to be diminished in the mutant cells.

This work demonstrates that changes in the induction curves of prompt and delayed fluorescence are among the first early detected parameters in microalgae after mutagenesis. These parameters can be effectively used for functional diagnostics of the objects examined. Our results are relevant to understanding the regulation of primary process in PSII and PSI, as well as for the use of fluorescence parameters in bioassays of water quality in natural and artificial reservoirs. In addition, the Chl *b*-free *C. reinhardtii* mutant CC-124y-1 is prospective for assessing the ecological status of contaminated aquatic ecosystems. The genetically determined test, i.e., pigment composition, provides an invaluable advantage for the use of this mutant in environmental monitoring aimed at assessment of mutability of the analyzed medium. The application of the proposed test organism enables an integrated assessment of the environment and improves the accuracy of predicting the long-term consequences of mutagenic contaminations.

## ACKNOWLEDGMENTS

We are grateful to Dr. E.P. Lukashev (Department of Biophysics, Moscow State University) for help with spectral measurements.

This work was supported by the Kazakh Foundation for Basic Research, project GF2015, no. 015RK00290) and by the Ministry of Education and Science of the Republic of Kazakhstan, project no. 1582/GF4.

## REFERENCES

- Zayadan, B.K. and Matorin, D.N., *Biomonitoring vodnykh ekosistem na osnove mikrovodoroslei* (Biomonitoring of Aquatic Ecosystems Based on Microalgae), Moscow: Al'teks, 2015.
- Sarapul'tseva, E., Geras'kin, S., and Tsatsenko, L.V., *Biologicheskii kontrol' okruzhayushchei sredy. Geneticheskii monitoring* (Biological Control of Environment. Genetic Monitoring), Moscow: Akademiya, 2010.
- Zayadan, B.K., Sadvakasova, A.K., Saleh, M.M., and Gaballah, M.M., Generation of pigment mutants of *Chlamydomonas reinhardtii* CC-124 and investigation of the mutants for evaluating the mutability of the waste water ecosystems, *Int. J. Curr. Microbiol. Appl. Sci.*, 2013, vol. 2, pp. 64–73.
- Zayadan, B.K., Sadvakasova, A.K., Saleh, M.M., and Gaballah, M.M., Generation and characterization of pigment mutants of *Chlamydomonas reinhardtii* CC-124, *Afr. J. Biotechnol.*, 2014, vol. 13, pp. 274–279.
- Strasser, R.J., Tsimilli-Michael, M., Qiang, S., and Goltsev, V., Simultaneous in vivo recording of prompt and delayed fluorescence and 820-nm reflection changes during drying and after rehydration of the resurrection plant *Haberlea rhodopensis*, *Biochim. Biophys. Acta*, 2010, vol. 1797, pp. 1313–1326.
- Gol'tsev, V.N., Kaladzhi, M.H., Kuzmanova, M.A., and Allahverdiev, S.I., *Peremennaya i zamedlennaya fluorestsentsiya khlorofilla a – teoreticheskie osnovy i prakticheskoe prilozhenie v issledovanii rastenii* (The Variable and Delayed Fluorescence of Chlorophyll *a* – Theoretic Basics and Practical Application in Plant Research), Moscow: Inst. Comput. Issled., 2014.
- Matorin, D.N. and Rubin, A.B., *Fluorestsentsii khlorofilla vysshikh rastenii i vodoroslei* (Chlorophyll Fluorescence in Higher Plants and Microalgae), Moscow: Inst. Comput. Issled. 2012.
- Bulychev, A.A., Osipov, V.A., Matorin, D.N., and Vredenbergh, W.J., Effects of far-red light on fluorescence induction in infiltrated pea leaves under diminished  $\Delta pH$  and  $\Delta\psi$  components of the proton motive force, *J. Bioenerg. Biomembr.*, 2013, vol. 45, pp. 37–45.
- Lenbaum, V.V., Bulychev, A.A., and Matorin, D.N., Effects of far red light on the induction changes of prompt and delayed fluorescence and the redox state of  $P_{700}$  in *Scenedesmus quadricauda*, *Russ. J. Plant Physiol.*, 2015, vol. 62, pp. 210–218.
- Matorin, D.N., Todorenko, D.A., Seifullina, N.Kh., Zayadan, B.K., and Rubin, A.B., Effect of silver nanoparticles on the parameters of chlorophyll fluorescence and  $P_{700}$  reaction in the green alga *Chlamydomonas reinhardtii*, *Microbiology*, 2013, vol. 82, pp. 809–814.
- Lazar, D. and Schansker, G., Models of chlorophyll *a* fluorescence transients, in *Photosynthesis in Silico*, Laisk, A., Nedbal, L., and Govindjee, Eds., Dordrecht: Springer-Verlag, 2009, pp. 85–123.
- Xue, L., Zhang, Y., Zhang, T., An, L., and Wang, X., Effects of enhanced ultraviolet-B radiation on algae and cyanobacteria, *Crit. Rev. Microbiol.*, 2005, vol. 31, pp. 79–89.
- Zayadan, B.K., Purton, S., Sadvakasova, A.K., Userbaeva, A.A., and Bolatkhan, K., Isolation, mutagenesis, and optimization of cultivation conditions of microalgal strains for biodiesel production, *Russ. J. Plant Physiol.*, 2014, vol. 61, pp. 124–130.
- Rastogi, R.P., Sinha, R.P., Moh, S.H., Lee, T.K., Kottuparambil, S., Kim, Y.J., Rhee, J.S., Choi, E.M., Brown, M.T., Häder, D.P., and Taejun, H., Ultraviolet radiation and cyanobacteria, *J. Photochem. Photobiol. B*, 2014, vol. 141, pp. 154–169.
- Moon, Y., Kim, S., and Chung, Y., Sensing and responding to UV-A in cyanobacteria, *Int. J. Mol. Sci.*, 2012, vol. 13, pp. 16 303–16 332.
- Han, C., Liu, Q., and Yang, Y., Short-term effects of experimental warming and enhanced ultraviolet-B radiation on photosynthesis and antioxidant defense of *Picea asperata* seedlings, *Plant Growth Regul.*, 2009, vol. 58, pp. 153–162.
- Voronova, E.N., Konyukhov, I.V., Kazimirko, Yu.V., Pogosyan, S.I., and Rubin, A.B., Changes in the condition of photosynthetic apparatus of a diatom alga *Thalassiosira weissflogii* during photoadaptation and photodamage, *Russ. J. Plant Physiol.*, 2009, vol. 56, pp. 753–760.

Translated by A. Bulychev